THE ASTROPHYSICAL JOURNAL, 543:313–317, 2000 November 1

INFRARED INTERFEROMETRIC OBSERVATIONS OF YOUNG STELLAR OBJECTS

R. L. AKESON,[1,2] D. R. CIARDI,[3] G. T. VAN BELLE,[2] M. J. CREECH-EAKMAN,[2] AND E. A. LADA[3]

Received 2000 February 22; accepted 2000 June 5

ABSTRACT

We present infrared observations of four young stellar objects made using the Palomar Testbed Interferometer (PTI). For three of the sources, T Tau, MWC 147, and SU Aur, the 2.2 μm emission is resolved at the PTI's nominal fringe spacing of 4 mas, while the emission region of AB Aur is overresolved on this scale. We fit the observations with simple circumstellar material distributions and compare our data to the predictions of accretion disk models inferred from spectral energy distributions. We find that the infrared emission region is tenths of an AU in size for T Tau and SU Aur and $\sim$1 AU for MWC 147.

Subject headings: circumstellar matter — stars: pre–main-sequence

1. INTRODUCTION

Observational evidence for circumstellar material around most young stellar objects (YSOs) includes infrared emission in excess of that expected from the stellar photosphere, broad forbidden line profiles, and emission at millimeter wavelengths. Although the dust column density is inferred to be quite high, the sources are often optically visible, implying a geometrically flat distribution of the material. A disk morphology is also predicted by star formation theories as a consequence of conservation of angular momentum. Evidence for circumstellar disks has been observed around sources with a range of masses, from near solar mass (T Tauri stars) to greater than 10 $M_\odot$ (Herbig Ae/Be stars; see, e.g., Mundy, Looney, & Welch 2000; Natta, Grinin, & Mannings 2000). Disks not only provide a conduit for material to accrete onto the central star but are also a reservoir of material from which a potential planetary system might form.

The structure of YSO circumstellar disks has been studied using spectral energy distributions (SED), spectral line profiles, and imaging at infrared and (sub)millimeter wavelengths. The dust continuum emission from disks around several T Tauri sources has been resolved at millimeter wavelengths (see review by Wilner & Lay 2000). These observations are sensitive to emission from cooler dust and provide spatial information on size scales of several tens of AU. The disk physical properties on much smaller scales (less than a few AU) are generally inferred through the examination of the spectral line shapes and modeling of the SED. Unresolved issues regarding the inner-disk structure include the possible existence of inner-disk holes (e.g., Hillenbrand et al. 1992) and the validity of simple power-law scalings to describe globally the temperature and density profiles of the disk. Characterizing the physical properties of the inner disk is important for theories of hydrodynamic disk winds and for understanding the initial conditions of planet formation.

Infrared interferometry provides a method to directly observe the inner disk. To date, only a few YSOs have been observed using this technique (e.g., FU Ori: Malbet et al. 1998 and AB Aur: Millan-Gabet et al. 1999). Here we present K-band long-baseline interferometric observations of four YSOs: T Tau, SU Aur, AB Aur, and MWC 147. The Palomar Testbed Interferometer (PTI) has a fringe spacing of $\sim$4 mas, which corresponds to 0.6 AU at the distance of Taurus-Aurigae (140 pc) and to 3 AU at the distance of MWC 147 (800 pc).

2. OBSERVATIONS AND DATA REDUCTION

Observations were made in the K band with the PTI, which are described by Colavita et al. (1999). The data were obtained between 1999 September and December. For each source, the number of nights, the total number of records (each of which contains 25 s of data), and the calibrators used are given in Table 1. The data were calibrated using the standard method described in Boden et al. (1998). A synthetic wideband channel is formed from the five spectrometer channels. The system visibility is measured with respect to the calibrators. The calibrator sizes were estimated using a blackbody fit to photometric data from the literature and were confirmed to be internally consistent when two or more calibrators were observed in a given night, which occurred on most nights. The calibrators were chosen by their proximity to the sources and for their small angular size, which minimizes systematic errors in deriving the system visibility. All calibrators used in this reduction have angular diameters less than 0.8 mas and were assigned uncertainties of 0.1 mas, except for HD 46709 ($\theta = 1.8 \pm 0.2$ mas). The data are presented in normalized squared visibility, which is an unbiased quantity. The averaged squared visibility and error are given for each source in Table 1. The uncertainties for the calibrated visibilities are a combination of the calibrator size uncertainty and the internal scatter in the data.

3. MODELS

Of the four objects discussed in this paper, three were resolved, and the fourth was overresolved (no fringes were detected). In this section we first detail the models and then discuss each source separately in the following section. The models fitted to the data are a uniform brightness profile, a Gaussian brightness profile, and a binary companion. We also compare the data to accretion disk models. The uniform and Gaussian profiles are presented as simple geometric distributions that can be used as size scale estima-

[1] Infrared Processing and Analysis Center, California Institute of Technology MS 100-22, 770 South Wilson Avenue, Pasadena, CA 91125.
[2] Jet Propulsion Laboratory, California Institute of Technology MS 171-113, 4800 Oak Grove, Pasadena, CA 91109.
[3] Department of Astronomy, University of Florida, P.O. Box 112055, 211 Bryant Space Sciences Building, Gainesville, FL 32611.

TABLE 1

PTI Observations

Source	Nights	Records	Calibrator (HD)	$\langle V^2 \rangle$	Uniform Disk Diameter[a] (mas)	Gaussian (FWHM)[a] (mas)
T Tau	4	119	28024, 27946	0.29 ± 0.01[b]	$2.62^{+0.046}_{-0.044}$	$1.61^{+0.028}_{-0.031}$
SU Aur	3	38	28024, 27946, 25867	0.68 ± 0.02	$1.92^{+0.063}_{-0.059}$	$1.16^{+0.038}_{-0.039}$
MWC 147.....	9	121	43042, 46709	0.53 ± 0.01	$2.28^{+0.017}_{-0.034}$	$1.38^{+0.013}_{-0.014}$
AB Aur	4[c]	...	32301	<0.15	>3.7	>2.4

[a] 1σ uncertainties are given for the best-fit Gaussian and uniform disk models.

[b] The visibility given for T Tau is the calibrated value uncorrected for the effects of T Tau S.

[c] Only nights with good upper limits are listed for AB Aur.

tors. At the distances to these systems (140–800 pc) the central star is unresolved ($\theta < 0.1$ mas). For the uniform and Gaussian distributions and the accretion disk models, a stellar component has been included as an unresolved source with the appropriate flux ratio. This ratio was determined by subtracting the photospheric flux of a star of the appropriate spectral type from the total K-band flux. For these objects, the infrared emission on milliarcsecond scales is dominated by thermal emission, and scattering can be neglected (Malbet & Bertout 1995).

3.1. *Uniform and Gaussian Profiles*

Two of the simplest geometric models that can be used to describe the circumstellar material distribution are a uniform brightness profile and a Gaussian profile. For a face-on Gaussian or uniform profile, the predicted visibility is simply a function of the projected baseline. For the uniform profile, the squared visibility is

$$V^2 = \left[\frac{2J_1(\pi\theta B_p/\lambda)}{\pi\theta B_p/\lambda}\right]^2, \quad (1)$$

where J_1 is a Bessel function, θ is the diameter, and B_p is the projected baseline. For a Gaussian profile,

$$V^2 = \left(\exp\left[-\frac{\pi^2}{\ln 2}\left(\frac{D}{2}\right)^2 \frac{B_p^2}{\lambda}\right]\right)^2, \quad (2)$$

where D is the FWHM.

For an inclined profile, the visibility is also a function of hour angle. As none of the sources show definitive visibility structure with hour angle, we limit ourselves to the simple face-on case. The observations cover hour angle ranges of -2^h to 2^h for T Tau, -2^h to 0 for SU Aur, and -3^h to 1^h for MWC 147. Although other inclinations and position angles are not necessarily excluded by the data, we note that inclination angles near edge-on would produce significant visibility variations with hour angle, which are not seen. The best-fit uniform and Gaussian profile sizes for each source are given in Table 1.

3.2. *Binary Companion*

A reduction from unity visibility can be produced by a binary companion. If both components are individually unresolved, the visibility is given by

$$V^2 = \frac{1 + R^2 + 2R\cos\left[(2\pi/\lambda)\boldsymbol{B}\cdot\boldsymbol{s}\right]}{(1+R)^2}, \quad (3)$$

where R is the flux ratio, $\boldsymbol{B}$ is the baseline vector, and $\boldsymbol{s}$ (in radians) is the binary angular separation vector. To test if the measured visibilities are consistent with a binary, a grid of binary parameters was formed, and model visibilities were calculated and compared to data binned by projected baseline. The binary parameter space considered contained primary/secondary flux ratios (R) from 1 to 30 and separations (s) up to 100 mas, which corresponds to the coherence length of the spectral channels. Binary companions beyond this separation with sufficient magnitude to affect the measured visibility have been ruled out by speckle or adaptive optics observations (T Tau and SU Aur: Ghez, Neugebauer, & Matthews 1993; MWC 147: Corporon 1998).

3.3. *Accretion Disk*

Emission from an accretion disk is one of the leading explanations for the infrared excess and other observed features of T Tauri stars and has also been proposed for Herbig Ae/Be stars. One common method of describing the physical properties of the accretion disk is to parameterize the temperature (T) and surface density (Σ) as power-law functions of the radius ($T \propto r^{-q}$, $\Sigma \propto r^{-p}$) and the dust opacity as a power-law function of wavelength ($\kappa \propto \lambda^{\alpha}$). At 2.2 μm the disk is optically thick, and the emission profile at a given radius depends on the temperature distribution (Beckwith et al. 1990). As we have only sampled one spatial scale in the disk, we will use accretion disk models from the literature, where the SED or millimeter imaging has been used to determine the disk parameters.

4. RESULTS

4.1. *T Tau*

T Tauri, one of the best-studied YSOs, has an infrared companion, T Tau S, 0.″7 to the south, which is optically obscured. Both components have a near-infrared excess, suggestive of circumstellar material. Recent observations have revealed that T Tau S is also a binary (Koresko 2000). The millimeter wave flux is dominated by material surrounding T Tau N and is consistent with circumstellar disk models with an outer radius of 40 AU (Akeson, Koerner, & Jensen 1998).

At K band, T Tau N is the component with higher flux, and thus it contributes the most to the measured visibility. The binary separation is sufficiently large such that the fringe envelopes of the two sources do not overlap, and thus T Tau S does not contribute any coherent flux. However, it is within the field of view of the star and fringe trackers and therefore contributes incoherent flux, reducing the observed V^2 on T Tau N by $R^2/(1+R)^2$, where R is the flux ratio between T Tau N and S. For these observations, the ratio has two components, the intrinsic K-band flux ratio of the system and an instrumental flux ratio introduced by an optical fiber, both of which are discussed below.

At PTI, the angle tracking passband is 0.7–1.0 μm. T Tau N is brighter than T Tau S in the visible. Stapelfeldt et al. (1998) measured a ratio of greater than 2000 in the I band; thus, the field will be centered on T Tau N. Since the optical path for the spectrometer channels includes a fiber with 1″ FWHM, the flux contribution from T Tau S is reduced. The relative coupling of the N/S flux was calculated in the following way: An Airy pattern given by the diffraction limit of 1.″2 was convolved with a 1″ Gaussian representing the seeing. We then used a matched filter of a Gaussian with 1″ FWHM for the fiber, which is centered on T Tau N. The errors were conservatively estimated by assuming the fiber FWHM to have an error of 50%. The resulting fiber coupling ratio (N/S) is 1.50 ± 0.2.

The total flux and flux ratio for the T Tau system varies on timescales of weeks to months (e.g., Skrutskie et al. 1996), and so roughly contemporaneous flux ratios are necessary. T. Beck (1999, private communication) measured a N/S flux ratio of 1.96 ± 0.19 on 1999 October 31. The last four nights of our data were taken on 1999 October 20 and 26 and November 2 and 3. In the analysis below, we assume that the flux ratio measured by Beck is valid for these four nights and use only these data.

We note that we have no direct way of knowing that the detected fringes arise from T Tau N instead of T Tau S. If the fringes do arise from T Tau S, then the expected visibility with T Tau S unresolved is $V^2 = 0.07$, much lower than that observed. The low visibility is due to the flux and fiber ratios still favoring T Tau N and would be even lower if T Tau S were resolved. The stability of the fringe tracking and the consistency of the night-to-night measurements strongly suggest that only one of the binary components is detected, and given the above argument, we deduce that T Tau N is the detected component.

To correct for T Tau S, the visibilities were divided by $R^2/(1 + R)^2$ before modeling was performed, where R represents the correction for both the intrinsic flux ratio, and the coupling effect described above and is 2.94 ± 0.48. For the stellar parameters estimated by Ghez et al. (1991) using optical photometry, the total to stellar flux ratio at K band is 3.6 for T Tau N. The stellar contribution is included in the models as an unresolved component. The visibilities show a slight dependence on hour angle, but more data are needed to confirm this effect.

The data were reduced and binned by projected baseline before being fitted by Gaussian and uniform profile models. The best-fit uniform profile diameter is $2.62^{+0.046}_{-0.044}$ mas (0.37 AU), and the best-fit Gaussian has an FWHM of $1.61^{+0.028}_{-0.031}$ mas (0.22 AU) (Fig. 1*a*). For the accretion disk model, we have used the parameters derived by Ghez et al. (1991) with $r_{\rm inner} = 0.04$ AU, $r_{\rm outer} = 100$ AU, a temperature profile of $T \propto r^{-0.42}$, and $T(1\,{\rm AU}) = 260$ K. This accretion disk model overestimates the measured visibility and thus underestimates the size scale. Using the disk parameters derived by Akeson et al. (1998) from millimeter wave emission [$r_{\rm inner} = 0.01$ AU, $r_{\rm outer} = 40$ AU, and $T \propto r^{-0.6}$, $T(1\,{\rm AU}) = 100$ K], the predicted size is even smaller than the Ghez model.

The binary parameters that fit the measured visibilities are shown in Figure 1*b*, where the contours are for χ^2_r of 1, 2, and 4. We note that if a binary companion at the separation shown in Figure 1*b* were in a roughly circular orbit around T Tau N, we should have seen visibility changes in the data given the time span covered by the observations. However, no time dependence was seen in the data.

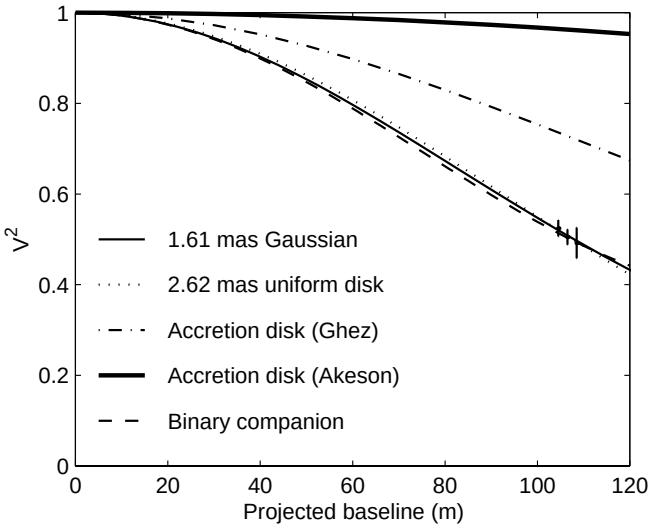

FIG. 1*a*

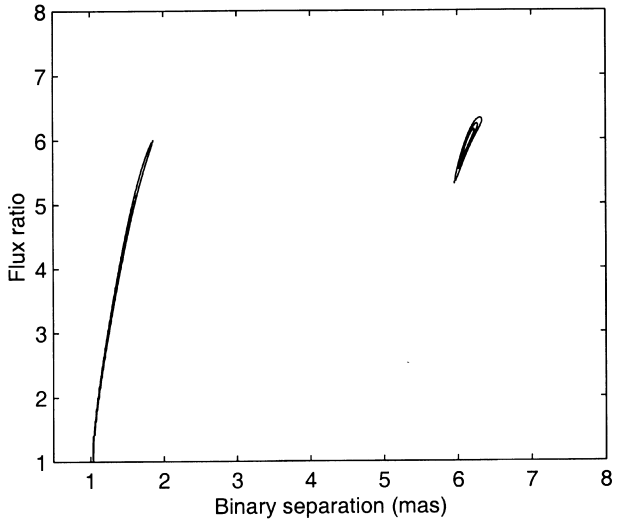

FIG. 1*b*

FIG. 1.—(*a*) Binned data and models for T Tau. The models are the Gaussian profile (*solid line*), uniform profile (*dotted line*), accretion disk from Ghez et al. (1991) (*dash-dotted line*), accretion disk from Akeson et al. (1998) (*thick solid line at top*), and binary companion (*dashed line*). The plotted visibilities have been corrected for the incoherent flux of T Tau S, as described in § 4.1. The binary parameters represented are separation of 1.5 mas and a flux ratio of 4.3. (*b*) Contour plot of possible binary companion parameters. The contour levels represent models with a χ^2_r of 1, 2, and 4.

4.2. *SU Aur*

SU Aur is a T Tauri star with an SED similar to that of T Tau. Herbig & Bell (1988) designated SU Aur as the prototype of a separate classification from weak-lined T Tauri stars because of its broad absorption lines and high luminosity ($\sim 12\ L_\odot$). The stellar/total flux ratio at K band is 0.3 (Marsh & Mahoney 1992). The best-fit diameters are $1.92^{+0.063}_{-0.059}$ mas and $1.16^{+0.038}_{-0.039}$ mas for a uniform profile and a Gaussian (FWHM), respectively (Fig. 2*a*). This corresponds to a physical size of 0.27 and 0.16 AU for a distance of 140 pc. The accretion disk model is taken from Beckwith et al. (1990) with $r_{\rm inner} = 0.01$ AU, $r_{\rm outer} = 100$ AU, a temperature profile $T \propto r^{-0.51}$, and $T(1\,{\rm AU}) = 260$ K, where

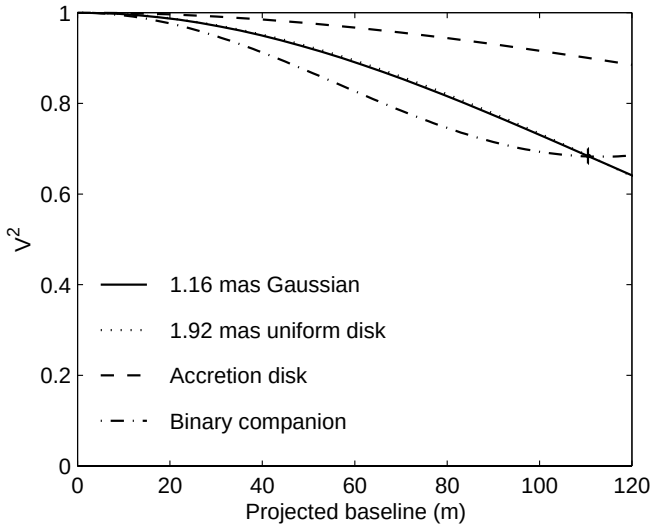

FIG. 2a

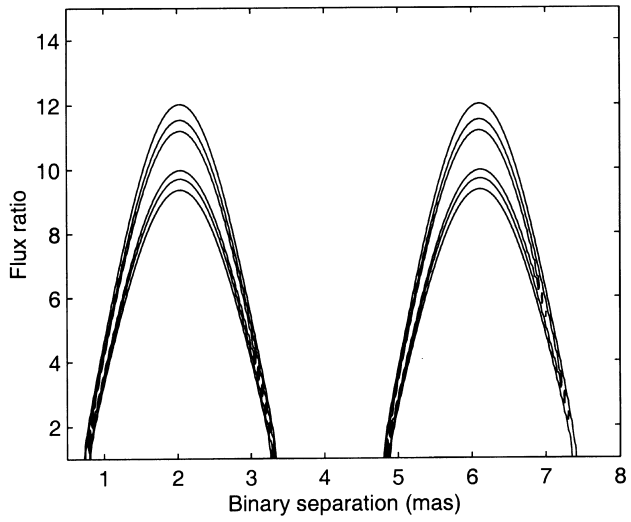

FIG. 2b

FIG. 2.—(*a*) Binned data and models for SU Aur. The models are the Gaussian profile (*solid line*), uniform profile (*dotted line*), accretion disk (*dashed line*), and binary companion (*dash-dotted line*). The binary parameters represented are a separation of 2 mas and a flux ratio of 10. (*b*) Contour plot of possible binary companion parameters. Note that this pattern repeats in separation space to 20 mas. The contour levels represent models with a χ_r^2 of 1, 2, and 4.

the parameters were determined by fitting 10 μm through millimeter wave fluxes. This model overestimates the observed visibility.

The binary parameter space for models with a reduced χ-squared, χ_r^2, of 1, 2, and 4 is shown in Figure 2*b*. The pattern shown in the figure repeats in separation space to roughly 20 mas. The binary companion hypothesis for SU Aur is not well constrained because of the limited time and baseline coverage of the data. The time coverage we do have favors orbiting companions with separations at roughly 2 or 6 mas.

4.3. *MWC 147*

MWC 147 (HD 259431) is a Herbig Ae/Be star with spectral classifications in the literature ranging from B2 to B6. Hillenbrand et al. (1992) modeled the SED from this source as arising from a flat, optically thick disk with an inner hole. Previous studies have used a distance to this source of 800 pc, which we will use here for consistency, although we note a recent distance determination from *Hipparcos* data of 290^{+200}_{-84} pc (Bertout, Robichon, & Arenou 1999). If the distance to MWC 147 is $\sim$290 pc, the physical sizes given below decrease by a factor of 2.8. Depending on which spectral type is used, the stellar contribution to the flux at K band is 0.05–0.1 of the total. We use an unresolved component with 0.1 of the total flux to represent the central star in these models. Using a stellar contribution of 0.05 would increase the squared visibility due to the disk by 4%.

The data were reduced as described above and binned by projected baseline. The data and models are shown in Figure 3*a*. Given the errors on the individual data points, there is no significant dependence on hour angle in the visibility data, consistent with Millan-Gabet (1999). The best-fit uniform profile diameter is $2.28^{+0.017}_{-0.034}$ mas (1.8 AU),

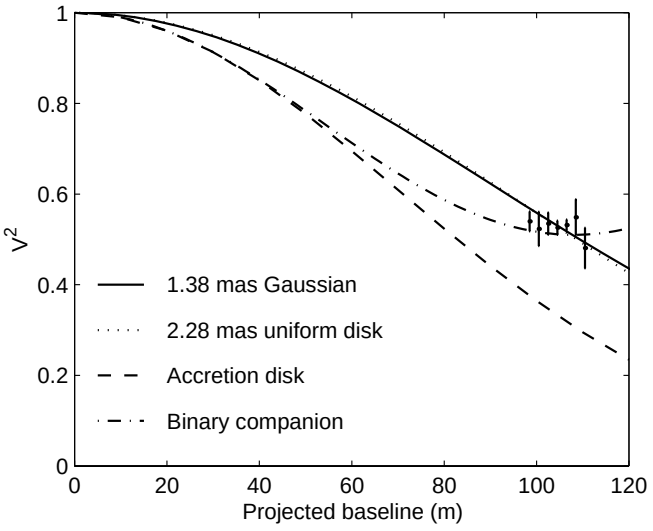

FIG. 3a

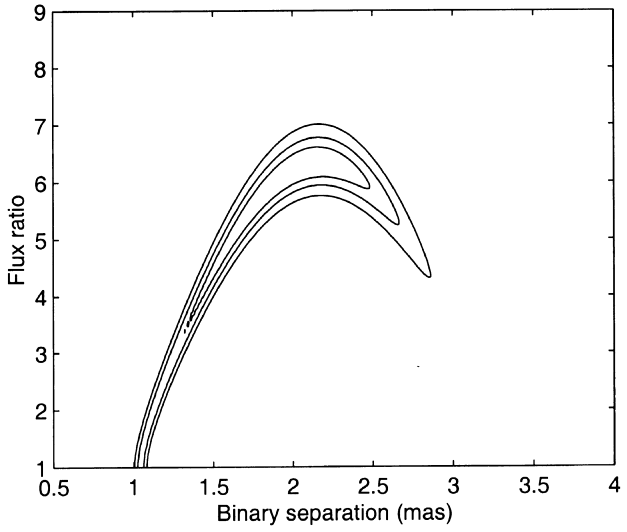

FIG. 3b

FIG. 3.—(*a*) Binned data and models for MWC 147. The models are the Gaussian disk (*solid line*), uniform disk (*dotted line*), accretion disk (*dashed line*), and binary companion (*dash-dotted line*). The binary parameters represented are a separation of 2.1 mas and a flux ratio of 6. (*b*) Contour plot of possible binary companion parameters. The contour levels represent models with a χ_r^2 of 1, 2, and 4.

and the best-fit Gaussian has an FWHM of $1.38^{+0.013}_{-0.014}$ mas (1.1 AU). The accretion disk and stellar parameters were taken from Hillenbrand et al. (1992), with $r_{\rm inner} = 0.36$ AU, $r_{\rm outer} = 1.8$ AU, and a temperature profile $T \propto r^{-3/4}$. The reference temperature is set by the stellar temperature, 2×10^4 K, and the accretion rate, $\dot{M} = 10^{-5}\ M_\odot\ {\rm yr}^{-1}$. As seen in Figure 3*a*, this accretion disk model underestimates the measured visibility and so overestimates the physical size.

The observed visibilities for MWC 147 can also be explained by a binary companion. Figure 3*b* shows the parameter space for binary models with a χ^2_r of 1, 2, and 4. An adaptive optics survey by Corporon (1998) found a binary companion to MWC 147 with a separation of 3".1 and a magnitude difference $\Delta K = 5.7$. This source is too widely separated and too faint to have affected our observations.

4.4. *AB Aur*

AB Aur is a Herbig Ae/Be star with a spectral type of A0 at a distance of 140 pc. Millan-Gabet et al. (1999) resolved the infrared emission from this source with the Infrared Optical Telescope Array interferometer using baselines of 21 and 38 m. At PTI, fringes were not detected on AB Aur, despite a photon flux higher than that for T Tau, indicating that the AB Aur is too large to be detected on baselines of $\sim$100 m with current sensitivities. Upper limits were found for the visibility using the sensitivity of the detection algorithm and measuring the system visibility with a calibrator. At K band the estimated upper limit was $\langle V^2 \rangle < 0.08 \pm 0.02$, which corresponds to a size greater than 4.1 ± 0.2 mas (0.57 AU) diameter for a uniform profile and greater than 2.7 ± 0.1 mas (0.38 AU) for a Gaussian. These results are consistent with the size derived by Millan-Gabet et al. (1999) and from a previous upper limit from PTI of $\langle V^2 \rangle < 0.3$ (Berger 1998).

5. DISCUSSION

The fundamental result of these observations is that for all four sources observed here the infrared emission arising from circumstellar material is resolved by PTI with a nominal fringe spacing of 4 mas. The measured sizes correspond to physical scales of tenths of an AU for the T Tauri sources T Tau and SU Aur and $\sim$1 AU for the Herbig Ae/Be star MWC 147. We note that if the correct distance for MWC 147 is 290 pc rather than 800 pc, then the measured visibility corresponds to a size scale of roughly 0.5 AU, similar to that measured for the T Tauri sources, despite the large difference in stellar mass. Our measured visibilities do not agree with those predicted from accretion disk models derived from near-infrared SEDs or millimeter interferometric observations. This may suggest that the single power-law relations used to describe the temperature and density are inadequate to reproduce both the spectral and spatial characteristics of the emission.

Our data on T Tau and SU Aur require the K-band emission to come from a larger region than that predicted by the accretion disk models, while the opposite is true for MWC 147. Millan-Gabet (1999) observed 15 Herbig Ae/Be stars using infrared interferometry with a shorter baseline and found that roughly half of the sources could not be well modeled as emission from an accretion disk and that the predicted visibilities were higher than the observed data. On the other hand, Malbet et al. (1998) used PTI for observations of FU Ori and found that an accretion disk model could explain the measured visibilities.

Further characterization of the circumstellar material on size scales less than 1 AU can be achieved by extending the infrared interferometry observations presented here. PTI has a second baseline, which provides data on shorter spacings, and is equipped to observe in the H band, which probes higher temperatures and has higher spatial resolution than K band. We plan to extend our study of young stellar objects to include H band and more spatial scales.

This work was performed at the Infrared Processing and Analysis Center, California Institute of Technology and the Jet Propulsion Laboratory. Data were obtained at the Palomar Observatory using the NASA Palomar Testbed Interferometer, which is supported by NASA contracts to the Jet Propulsion Laboratory. Science operations with PTI are possible through the efforts of the PTI Collaboration (http://huey.jpl.nasa.gov/palomar/ptimembers.html). We particularly thank A. Boden for his efforts in data reduction software and B. Thompson for useful discussions. We are also grateful to T. Beck for providing the T Tau flux ratio. D. R. C. acknowledges support from NASA WIRE ADP NAG 5-6751. E. A. L. acknowledges support from a Research Corporation Innovation Award and a Presidential Early Career Award for Scientists and Engineers to the University of Florida.

REFERENCES

Akeson, R. L., Koerner, D. W., & Jensen, E. L. N. 1998, ApJ, 505, 358
Beckwith, S. V. W., Sargent, A. I., Chini, R. S., & Gusten, R. 1990, AJ, 99, 924
Berger, J. P. 1998, Ph.D. thesis, Univ. Joseph Fourier de Grenbole
Bertout, C., Robichon, N., & Arenou, F. 1999, A&A, 352, 574
Boden, A. F., Colavita, M. M., van Belle, G. T., & Shao, M. 1998, Proc. SPIE, 3350, 872
Colavita M. M., et al. 1999, ApJ, 510, 505
Corporon, P. 1998, Ph.D. thesis, Univ. Joseph Fourier de Grenbole
Ghez, A. M., Neugebauer, G., Gorham, P. W., Haniff, C. A., Kulkarni, S. R., Matthews, K., Koresko, C., & Beckwith, S. 1991, AJ, 102, 2066
Ghez, A. M., Neugebauer, G., & Matthews, K. 1993, AJ, 106, 2005
Herbig, G. H., & Bell, K. R. 1988, Lick Obs. Bull. 111
Hillenbrand, L. A., Strom, S. E., Vrba, F. J., & Keene, J. 1992, ApJ, 397, 613
Koresko, C. D. 2000, ApJ, 531, L147
Malbet, F., et al. 1998, ApJ, 507, L149
Malbet, F., & Bertout, C. 1995, A&AS, 113, 369
Marsh, K. A., & Mahoney, M. J. 1992, ApJ, 395, L115
Millan-Gabet, R. 1999, Ph.D. thesis, Univ. Massachusetts
Millan-Gabet, R., Schloerb, F. P., Traub, W. A., Malbet, F., Berger, J. P., & Bregman, J. D. 1999, ApJ, 513, L131
Mundy, L. G., Looney, L. W., & Welch, W. J. 2000, in Protostars and Planets IV, ed. V. Mannings, A. P. Boss, & S. S. Russell (Tucson: Univ. Arizona Press), 355
Natta, A., Grinin, V. P., & Mannings, V. 2000, in Protostars and Planets IV, ed. V. Mannings, A. P. Boss, & S. S. Russell (Tucson: Univ. Arizona Press), 559
Skrutskie, M. F., Meyer, M. R., Whalen, D., & Hamilton, C. 1996, AJ, 112, 2168
Stapelfeldt, K. R., et al. 1998, ApJ, 508, 736
Wilner, D. J., & Lay, O. P. 2000, in Protostars and Planets IV, ed. V. Mannings, A. P. Boss, & S. S. Russell (Tucson: Univ. Arizona Press), 509